

1      **Ozone Design Values in Southern California's Air Basins:**  
2      **Temporal Evolution and U.S. Background Contribution**

3              David D. Parrish<sup>1,2</sup>, Lindsay M. Young<sup>2,3</sup>, Mia H. Newman<sup>2,4</sup>, Kenneth C. Aikin<sup>1,2</sup>,

4    Thomas B. Ryerson<sup>2</sup>

5              <sup>1</sup>Cooperative Institute for Research in Environmental Sciences, University of Colorado, Boulder,  
6              USA

7              <sup>2</sup>NOAA/ESRL Chemical Sciences Division, Boulder, Colorado, USA

8              <sup>3</sup>Now at East High School, Denver, Colorado, USA

9              <sup>4</sup>Now at Ralston Middle School, Belmont, California, USA

10

11      **Key points:**

- 12              • The temporal evolution of maximum ozone concentrations in southern California is  
13    accurately described by a simple mathematical function.
- 14              • The U.S. background ozone contribution of  $62.0 \pm 1.9$  ppb is the lower limit achievable  
15    for the concentrations upon which the NAAQS is based.
- 16              • Projections indicate ~35 years of additional emission control efforts will be required to  
17    reach the NAAQS in the Los Angeles area.

18     **ABSTRACT:** California's ambient ozone concentrations have two principal contributions: U.S.  
19     background ozone and enhancements produced from anthropogenic precursor emissions; only  
20     the latter effectively respond to California emission controls. From 1980-2015 ozone has been  
21     monitored in eight air basins in Southern California. The temporal evolution of the largest  
22     measured concentrations, i.e. those that define the ozone design value (ODV) upon which the  
23     National Ambient Air Quality Standard (NAAQS) is based, is described very well by an  
24     exponential decrease on top of a positive offset. We identify this offset as the ODV due to the  
25     U.S. background ozone (i.e., the concentration that would be present if U.S. anthropogenic  
26     precursor emissions were reduced to zero), and is estimated to be  $62.0 \pm 1.9$  ppb in six of the  
27     basins. California's emission control efforts have reduced the anthropogenic ozone  
28     enhancements by a factor of  $\sim 5$  since 1980. However, assuming that the current rate of  
29     exponential decrease is maintained and that U.S. background ODV remains constant, projections  
30     of the past decrease suggests that  $\sim 35$  years of additional emission control efforts will be  
31     required to reach the new NAAQS of 70 ppb in the Los Angeles area. The growing  
32     predominance of U.S. background ozone contributions has shifted the maximum ozone  
33     concentrations in all air basins from later to earlier in the summer. Comparisons indicate that  
34     currently accepted model estimates of U.S. background ozone concentrations in southern  
35     California are somewhat underestimated; thus reducing ozone in this region to the 2015 NAAQS  
36     may be more difficult than currently expected.

38    **1. Introduction**

39    In 1970 the U.S. passed the Clean Air Act, which required states to develop plans to improve  
40    air quality. Since its introduction, comprehensive efforts have been made to reduce emissions of  
41    the ozone precursors, oxides of nitrogen ( $\text{NO}_x = \text{NO} + \text{NO}_2$ ) and volatile organic compounds  
42    (VOCs), in order to meet the ozone National Ambient Air Quality Standard (NAAQS). The  
43    resulting emission reductions have produced substantial decreases in ambient ozone  
44    concentrations throughout the Nation, including southern California, which is the focus of this  
45    work. Quantification of these decreases and comparison of the decreases between different  
46    regions can potentially provide useful information for 1) partitioning ambient ozone  
47    concentrations between that produced locally and regionally from that transported from  
48    elsewhere, 2) forecasting likely possible evolution of these concentrations, 3) providing metrics  
49    for evaluating photochemical models designed to reproduce ambient ozone concentrations, and  
50    4) determining the most effective approach for further reducing the concentrations. Our goal in  
51    this paper is to develop a mathematical description of the temporal evolution of the maximum  
52    observed ozone concentrations in southern California, and to discuss the implications of the  
53    results.

54    The ozone NAAQS is based on the relatively rare, highest observed ozone concentrations, i.e.  
55    the 4th highest maximum daily 8-hour average (MDA8) ozone concentration measured in a  
56    given year at a sampling site. The Ozone 8-Hour Design Value (ODV) is defined as the 3-year  
57    running mean of this 4th highest annual concentration; it must not exceed the ozone NAAQS,  
58    currently set at 70 ppb. Assuming that the highest ozone concentrations occur during the 6-  
59    month (May - October) warm season, the 4th highest represents approximately the 98th  
60    percentile of the observed MDA8 ozone concentrations. The ODV is calculated each year for

61 each monitoring site with measurements over that year and the preceding two years that meet  
62 completeness criteria. The ODV is defined each year for each of southern California's eight air  
63 basins (Figure 1) as equal to the largest ODV for any site within the basin. Our primary focus is  
64 on these basin ODVs.

65 One challenge to meeting the ozone NAAQS is that ozone transported into the U.S. from  
66 outside its borders contributes a significant fraction to the total ambient concentrations (*Lin et*  
67 *al.*, 2015a; *Cooper et al.*, 2015). This contribution does not effectively respond to reductions in  
68 U.S. ozone precursor emissions, but does significantly reduce the margin for locally and  
69 regionally produced ozone before the NAAQS is exceeded. In this work, and consistent with  
70 other references (e.g., *U.S. EPA* 2015), we identify this transported component plus any ozone  
71 produced from local natural emissions as U.S. background ozone, i.e., the concentration that  
72 would be present if U.S. anthropogenic emissions of ozone precursors were reduced to zero. The  
73 analysis presented in this paper provides an estimate for the lowest NAAQS that could possibly  
74 be achieved in southern California's air basins by reducing U.S. anthropogenic ozone precursor  
75 emissions to zero, leaving only the U.S. background concentrations. We refer to this lowest  
76 NAAQS as the U.S. background ODV.

77 Other terms have been used to quantify the ozone concentrations transported into the U.S. We  
78 will also refer to baseline ozone concentrations (*Cooper et al.*, 2015), which are those completely  
79 unaffected by continental influences. They can be directly measured at sites sufficiently isolated  
80 such that the ozone transported ashore from the Pacific arrives without significant perturbation  
81 from continental influences. U.S. background ozone concentrations (as defined by the U.S. EPA  
82 and used in this work) differ from baseline ozone concentrations, because the former are affected  
83 by continental influences, including deposition to continental surfaces, especially vegetation, and

84 production from natural ozone precursors, such as those emitted from soils, trees and lightning;  
85 the U.S. background ozone concentrations thus vary with location throughout the U.S. depending  
86 on the influence of these continental effects. Additional definitions of background ozone will be  
87 discussed when we compare our results with modeling results in a later section of this paper.

88 An important characteristic of baseline ozone concentrations transported into California is their  
89 strong dependence on altitude. Figure 1 shows this altitude dependence at Trinidad Head, which  
90 is on the California coast approximately 300 km north of the top edge of the map in Figure 1.

91 The strong vertical gradient below about 1 km is caused by relatively rapid photochemical  
92 destruction of ozone in the humid marine boundary layer (MBL), where the concentrations of  
93 ozone precursors are sufficiently low that photochemical ozone formation cannot compensate for  
94 destruction (e.g., Ayers *et al.*, 1992; Oltmans and Levy, 1992; 1994). Importantly, baseline  
95 ozone at 2 km altitude is  $53 \pm 15$  ppb (average  $\pm 1$  standard deviation), so that baseline ozone  
96 often approaches the NAAQS of 70 ppb at this altitude. Although Trinidad Head is located north  
97 of the region considered in this work, these results are representative of southern California  
98 baseline ozone, because there is very little latitudinal variation in average baseline ozone  
99 concentrations along the California coast (Pfister *et al.*, 2011).

100 Our analysis in this paper examines the temporal evolution of the ODVs in the eight air basins  
101 defined for southern California (Figure 1). We choose to focus on this region for three reasons:  
102 first, the largest ozone concentrations in the nation have been, and continue to be, observed here;  
103 second, the prevailing winds are from the Pacific Ocean, so that air transported into the region  
104 largely brings baseline ozone concentrations relatively unaffected by ozone produced elsewhere  
105 in the U.S., so that interpretation of ozone concentrations is less complicated than in other U.S.  
106 regions; and third, ozone measurements have been made over the past several decades

107 throughout the region. We first develop a mathematical description of the evolution of the  
108 ODVs for the southern California air basins, and then discuss the implications of this description.

109 **2. Methods and Results**

110 Three approaches are used to investigate the temporal trends of the ODVs in the Southern  
111 California air basins. Our first task is to define for each air basin the set of basin ODVs to be  
112 examined (Section 2.1). The first analysis approach applies a general mathematical functional  
113 form to approximate the temporal ODV trends for the individual air basins in Southern  
114 California (Section 2.2). The second analysis compares the temporal trends in different air  
115 basins by means of correlations of ODVs between air basins (Section 2.3). Finally, a  
116 multivariate, least-squares analysis provides as complete a description as possible for the  
117 temporal evolution of the ODVs in seven of the southern California air basins (Section 2.4). The  
118 results of this third analysis will provide the primary basis for the discussion in Section 3.

119 **2.1. Selection of Air Basin Ozone Design Values**

120 For air quality monitoring and policy development, southern California has been divided into  
121 eight air basins (Figure 1). Routine monitoring of ambient ozone concentrations began in the  
122 late 1960s in the South Coast Air Basin and was rapidly expanded to the other basins. The  
123 California Air Resources Board (CARB) maintains a publicly accessible archive  
124 (<https://www.arb.ca.gov/adam/index.html>) of ODVs calculated from the results of this  
125 monitoring for all of California's individual monitoring sites and air basins for the years 1975 -  
126 2015. In this work we use these ODVs to examine the temporal evolution of ozone  
127 concentrations in the Southern California air basins.

128       The temporal evolution of the ODVs in a given air basin is affected not only by temporal  
129       changes in the ozone concentrations within the air basin, but also by changes in the monitoring  
130       sites that are operational in the basin. We wish to investigate the former without obscuring  
131       effects from the latter, so we must control for monitoring sites beginning or ending  
132       measurements over the measurement record. Figures S1-S8 illustrate the basin ODVs and show  
133       the ODVs from the sites that determine each basin's ODV in each year. Maps are included  
134       showing the locations of those sites in three air basins. In most basins, maximum ODVs were  
135       reached by 1980, so our analysis begins in that year when possible. In two air basins, North  
136       Central Coast and Mojave Desert (Figures S4 and S5), the ODVs in 1989 and 1987, respectively,  
137       were significantly higher than observed in previous years; these increases in observed ozone  
138       were due to recently initiated sites, so we begin analysis for these two air basins in those years.  
139       In one air basin (South Central Coast, Figure S3) in 1986 the site ODVs are missing from the  
140       two Simi Valley sites that determine the basin ODV in nearly all other years, so 1986 is excluded  
141       from the analysis of this site. Finally, monitoring began later in the Great Basin Valleys Air  
142       Basin (Figure S8) so ODVs are not available until 1986. As summarized in Table 1, our analysis  
143       considers all ODVs for the eight air basins from 1980 to 2015, with the exceptions discussed  
144       above.

145       In addition to the ODVs we will also investigate the dates of each year that the highest MDA8  
146       ozone concentrations were recorded in each of the eight Southern California air basins. This  
147       analysis will include both the four highest and the thirty highest MDA8 concentrations. The  
148       former are available from the publicly accessible archive given above; the latter were provided to  
149       us through a request to CARB staff.

150       **2.2. Mathematical Description of Temporal Evolution of Air Basin Ozone Design Values**

151 In each of the eight southern California air basins ozone concentrations have significantly  
152 decreased as is evident in Figures S1-S8. An exponential function with a constant positive offset  
153 (Equation 1) is used to quantify the temporal evolution of the ODVs in each air basin:

$$154 \quad ODV = y_0 + A \exp\{-(year-1980)/\tau\}. \quad (1)$$

155 Mathematically, the first term,  $y_0$ , is the asymptotic value toward which the basin ODVs are  
156 approaching, and the second term is the enhancement of the ODVs above  $y_0$ , which is assumed to  
157 be decreasing exponentially with an e-folding time constant of  $\tau$  years. Thus,  $A$  is the  
158 enhancement of the ODVs above  $y_0$  in 1980. A least-squares fitting routine is used to fit  
159 Equation 1 to any time series of ODVs.

160 If the time evolution of the ODVs for an air basin followed Equation 1 exactly, then a least-  
161 squares fit could accurately and precisely determine the three parameters  $y_0$ ,  $\tau$ , and  $A$ . However,  
162 deviations from Equation 1, resulting from interannual variability or other "noise" in the ODVs,  
163 generally prevent a precise determination of all three parameters from a single regression fit.

164 Consequently, we apply the following procedure to derive estimates of all three parameters.  
165 First, three-parameter fits were examined for the ODVs, as well as for several percentiles of the  
166 MDA8 ozone concentrations, in many of the air basins (Figure 2 of *Parrish et al., 2016a* give  
167 some example fits). In favorable cases, relatively precise determinations of all three parameters  
168 are possible. In these cases, all determinations of  $\tau$  agreed within their 95% confidence limits,  
169 although some of the confidence limits were quite wide. The weighted average of all of the  
170 results was  $22.3 \pm 4.0$  years (95% confidence limits are indicated here and elsewhere), which is  
171 taken as the initial best estimate for the value of  $\tau$ . This best estimate is assumed to apply to all  
172 of the air basins; the validity of this assumption will be discussed in the analysis that follows.  
173 Substitution of this value of  $\tau$  into Equation 1 allows the other two parameters,  $y_0$  and  $A$ , to be

174 determined for any particular time series of ODV values. Figures S1-S6 and Figure 2 show these  
175 two-parameter fits for the six southern California air basins whose ODVs have evolved  
176 approximately as described by Equation 1, and the derived parameters are given in Table 1. Also  
177 included in the table are root-mean-square deviations in ppb ( $\sigma$ ) between the observed ODVs and  
178 the derived fits. Note that the North Central Coast Air Basin has relatively small observed trends  
179 in the ODVs, which leads to large relative uncertainties in even the two-parameter fit. To  
180 improve the precision of the  $A$  determination for this air basin,  $y_0$  is set equal to that derived for  
181 the adjacent South Central Coast Air Basin, i.e. 62.9 pbbv.

182 The success of the quantification of the ODV evolution by Equation 1 in each air basin can be  
183 evaluated by examining the second term on the right side of Equation 1 (i.e., subtracting the  
184 derived  $y_0$  value from the observed ODVs) on a logarithmic scale; Figure 3 presents this  
185 evaluation for the same six air basins considered in Figure 2. In this format, linear regressions to  
186 the data give the values of  $\tau$  and  $A$  for each air basin as the inverse of the slopes and the inverse  
187 log of the 1980 intercepts, respectively. Table 2 gives the results of this analysis; here the  $\sigma$   
188 values give the relative root-mean-square deviation (in %) between the ODV enhancements and  
189 the derived fits.

190 The analyses illustrated in Figures 2 and 3 provide an excellent mathematical description of the  
191 temporal evolution of the ODVs in all six air basins. The large  $r^2$  values included in Table 2 ( $\geq$   
192 0.95 except for the North Central Coast where the enhancements above  $y_0$  are relatively small)  
193 indicate that the fit to Equation 1 captures the large majority of the total variance in the data sets  
194 (approximately equal to  $r^2$ ); the root-mean-square deviations are also small (3 to 5 ppb)  
195 compared to the range of observed ODVs (~ 200 ppb) shown in Figure 2. In all cases the  
196 derived values of  $\tau$  agree within the indicated confidence limits with the originally assumed

197 value of 22.3 years, and the values of  $A$  similarly agree between the two analyses. This  
198 agreement of  $\tau$  and  $A$  is expected, since the analysis illustrated in Figure 3 requires the  $y_0$  values  
199 derived in the fitted curves illustrated in Figure 2. One interesting result indicated in Table 1 is  
200 the agreement of  $y_0$  within their statistical uncertainties between five of the air basins (58 to 64  
201 ppb); only  $y_0$  for the Salton Sea Air Basin (76 ppb) is significantly greater than the range of the  
202 other five.

203 The uncertainties indicated for the derived parameter values in Tables 1 and 2 and elsewhere in  
204 this paper are estimated 95% confidence limits derived from the least squares regression  
205 analyses. It should be noted that since the ODVs are the 3-year running means of 4th highest  
206 MDA8 ozone concentration measured in a given year at a particular sampling site, the ODVs  
207 have a significant degree of autocorrelation. This serves to reduce the number of statistically  
208 independent ODV values (i.e., the degree of freedom) of a data set by as much as a factor of 3  
209 from the number of years included in the data set. In all cases the tabulated 95% confidence  
210 limits are a factor of  $\sqrt{3}$  greater than the confidence limits returned from the least squares  
211 analyses in order to properly account for this reduction in the degrees of freedom due to this  
212 autocorrelation.

213 **2.3. Correlation of Ozone Design Values between Air Basins.**

214 A somewhat different and more general approach can be applied to define the temporal trends  
215 of the ODVs of seven of the southern California air basins. This approach is based upon  
216 correlation of the ODVs from other basins with those of the South Coast Air Basin. In this  
217 approach, defining a functional form for the temporal evolution of the ODVs (such as given in  
218 Equation 1) is not required. The South Coast Air Basin is selected as a reference because  
219 Equation 1 most closely fits the temporal trend of that basin's ODVs, as indicated by the  $r^2$  value

220 of 0.99 obtained from the linear regression in Figure 3. Figures S9-S15 and Figure 4 illustrate  
221 the correlations of the basin ODVs; the supplemental figures indicate the years of data included  
222 in Figure 4. A reduced major axis regression procedure gave the linear fits. In these fits the x  
223 and y variables were weighted equally with that weighting based on an assumed 2.6 ppb 1-sigma  
224 uncertainty for ozone in all basins; this uncertainty was calculated from a representative root-  
225 mean-square deviation of data from the fits in the figures. The intercept and the slope of each  
226 correlation (which are annotated in Figures S9-S15) provide second determinations of the  $y_0$   
227 value and the  $A$  value of the respective air basin. The vertical dotted lines in Figure 4 indicate  
228 the  $y_0$  value of 58.9 ppb derived for the South Coast Air Basin, so the intercept of each linear fit  
229 with this vertical line provides an estimate of the corresponding  $y_0$  value for that basin. The  
230 slope of each correlation provides an estimate of the ratio of the corresponding  $A$  value to that of  
231 the South Coast Air Basin. Table 3 gives the results of this analysis.

232 The results in Table 3 are nearly identical to the previous results included in Tables 1 and 2, so  
233 this correlation approach simply provides another consistency test for the six air basins included  
234 in the earlier analysis. Here again the large  $r^2$  values ( $\geq 0.95$  except for the North Central Coast)  
235 indicate that correlation of a basin's ODVs with those of the South Coast Air Basin provides an  
236 excellent mathematical description of the temporal evolution of those ODVs. In addition, this  
237 correlation approach allows the investigation of two additional air basins that are not well  
238 described by Equation 1. Figure 4b includes all of the ODVs from the Great Basin Valleys Air  
239 Basin; a weak correlation with the South Coast Air Basin is apparent ( $r^2 = 0.38$ ), but the  
240 significance of the derived parameters is not clear; the temporal evolution of the ODVs in this air  
241 basin will not be considered further. Figure S7 and S14 show that before the year 2000, the  
242 ODVs in the San Joaquin Valley Air Basin decreased quite slowly with only a weak correlation

243 ( $r^2 = 0.28$ ), with the ODVs of the South Coast Air Basin. However, after 2000 the San Joaquin  
244 Valley ODVs decreased much more rapidly, and with a good correlation ( $r^2 = 0.94$ ) with the  
245 ODVs of the South Coast Air Basin. For the San Joaquin Valley Air Basin, the ODVs included  
246 in Figure 4, the results in Table 3 and the following discussion only include the period after  
247 2000.

248 Despite the close agreement in magnitude of the parameters in Tables 1 and 3, the confidence  
249 limits are systematically smaller in the latter. The analysis based on Equation 1 compares the  
250 data of each basin to that exponential function, and calculates the uncertainty of the derived  
251 parameters from the scatter of the data about the curve defined by Equation 1. The results in  
252 Table 3 are derived from the correlation between each basin's data with the South Coast Basin  
253 data. Some of the interannual variability in each basin's data correlates with the interannual  
254 variability in the South Coast data. This correlation reduces the scatter of the data about the  
255 linear fits in Figures S9-S15, resulting in a reduced uncertainty in the parameters derived in  
256 Table 3. Importantly, neither of these approaches captures the full uncertainty of the derived  
257 parameters, because both approaches assume an exact value of one critical parameter; the first  
258 approach sets  $\tau = 22.3$  years, and the second approach sets  $y_0 = 58.9$  ppb for the South Coast Air  
259 Basin. The multivariate approach described in the next section does not have this limitation, as  
260 the values of all parameters of Equation 1 are derived simultaneously.

261 The correlation analysis developed in this section reinforces the conclusion of the previous  
262 section that Equation 1 provides an excellent description of the temporal evolution of the basin  
263 ODVs. Notably, the correlations for five of the air basins with the South Coast Air Basin all  
264 intersect the vertical dotted line at ODVs that correspond to an average  $y_0$  value of 61.8 ppb for

265 the six air basins; only the Salton Sea Air Basin has a significantly higher ( $76 \pm 5$  ppb) intercept  
266 and corresponding  $y_0$  value.

267 **2.4. Multivariate Least-Squares Analysis of Ozone Design Values in Seven Air Basins**

268 The results from the preceding sections summarized in Tables 1-3 show a great deal of  
269 consistency between analyses as well as similarity between seven air basins. The ODVs in all air  
270 basins are approaching the same asymptote,  $y_0$  (within the statistical confidence limits), except in  
271 the Salton Sea Air Basin where the ODVs are approaching a significantly higher value. A single  
272 e-folding time,  $\tau = 22.3$  years, fits the temporal evolution of each basin, and the  $\tau$  results derived  
273 from Figure 3 and given in Table 2 agree with this value within the statistical confidence limits.  
274 Finally, each basin has its own distinct value of  $A$  that agrees in all three analyses within the  
275 statistical confidence limits.

276 In this section we simultaneously optimize the parameters describing the ODV temporal  
277 evolution in all southern California air basins (excluding the Great Basin Valleys Air Basin) for  
278 all years given in Table 1, except only after year 2000 in San Joaquin Valley Air Basin; this  
279 selection provides 214 total data points. The optimization approach iteratively varied the  
280 parameters of Equation 1 for each air basin to optimize the fit for the entire data set in a process  
281 following that described in Chapter 8 of *Bevington and Robinson* [2003]. More details of this  
282 multivariate analysis are given in the Supporting Information. In principle, this process can  
283 derive separate values with confidence limits for  $A$ ,  $\tau$  and  $y_0$  for each of the seven air basins for a  
284 total of 21 parameter values. However, in practice only ten distinct parameters were necessary to  
285 describe nearly all of the systematic variance in the ODV data set. These ten parameter values  
286 are consistent with the previous analyses: a single  $\tau$ , a common  $y_0$  for six basins plus a separate  $y_0$   
287 for the Salton Sea Air Basin, and seven values of  $A$ , one for each of the seven air basins. Table 4

288 gives the results of this analysis and Figure 5 compares the observed ODVs with those calculated  
289 from the derived parameters. While the results of this multivariate analysis agree with those  
290 from the previous analyses, simultaneous consideration of all data provides significantly smaller  
291 confidence limits, indicating a more precise determination of all parameter values. The square of  
292 the correlation coefficient ( $r^2 = 0.984$ ) provides an estimate of the fraction of the variance in the  
293 total log-transformed data set that is captured by the ten derived parameters; this large  $r^2$  value  
294 indicates that Equation 1 with the parameters of Table 4 provides an excellent description of the  
295 temporal evolution of the ODVs in all seven air basins.

296 Two further aspects of the multivariate analysis should be noted. First, the results for the San  
297 Joaquin Valley Air Basin are based on 2001-2015 ODVs. The value of  $A$  given in Table 4 (and  
298 in Table 3) is indicated in parentheses because  $A$  indicates the 1980 ODV enhancement above  $y_0$ ,  
299 but the ODVs in this air basin followed a very different temporal evolution from 1980 to 2000  
300 (see Figure S7); thus the indicated  $A$  value has no relation to the actual ODV in 1980 in that air  
301 basin. For the other six air basins the indicated  $A$  values do give fits to the actual or extrapolated  
302 ODV enhancement in 1980. Second, the remaining fraction of the variance of the data (~1.6%)  
303 not captured by the multivariate analysis with ten parameters is largely due to interannual  
304 variability and other noise about the regression fit. Attempts to extract more information from  
305 the data set (i.e., inclusion of additional parameters to capture additional systematic differences  
306 in  $y_0$  or in  $\tau$  between air basins) give results that fail to converge or converge to physically  
307 unreasonable results. In summary, the results in Table 4 are believed to provide all of the  
308 statistically significant information regarding the temporal evolution of the ODVs in the seven  
309 air basins over the time periods considered. However, it may become possible to extract further  
310 information as additional years of ozone monitoring data become available.

311    **3. Discussion**

312    **3.1. Physical Interpretation of Derived Parameters**

313    The analysis in the preceding section is purely mathematical; it shows that Equation 1 with the  
314    ten parameters included in Table 4 gives an excellent description of the temporal evolution of the  
315    air basin ODVs in southern California, but provides no physical basis for that equation. In this  
316    section we discuss this physical basis, and provide hypotheses for the physical interpretation of  
317    the ten parameters.

318    The long-term decrease in ODVs in southern California is the result of emission control efforts  
319    that have reduced ambient concentrations of ozone precursors by large fractions. In the five  
320    decades from 1960 to 2010 the ambient volatile organic carbon (VOC) concentrations in the Los  
321    Angeles region were reduced by about 98% (i.e., a factor of ~50) (*Warneke et al.*, 2012), and the  
322    concentrations of ambient nitrogen oxides (NO<sub>x</sub>) were reduced by about 75% (i.e., a factor of  
323    ~4) (*Pollack et al.*, 2013; *Parrish et al.*, 2016a). These large fractional reductions of the primary  
324    precursors of photochemical ozone production suggest that extrapolation of the past ozone  
325    decrease through the imagined elimination of the relatively small remaining fraction of  
326    anthropogenic emissions provides a quantification of the ODVs resulting solely from U.S.  
327    background ozone concentrations. Thus, we identify the parameter  $y_0$  (the asymptote toward  
328    which the ODVs are converging) as an estimate of the U.S. background ODV, i.e., the minimum  
329    ODV that could be achieved in a given air basin if US background ozone concentrations were  
330    not enhanced by North American anthropogenic emissions.

331    In each of California's air basins, emissions of ozone precursors from U.S. anthropogenic  
332    sources provide fuel for local and regional photochemical production of ozone that increases the  
333    ODV above  $y_0$ . Thus, the parameter  $A$  is interpreted as the magnitude of the enhancement of the

334 ODV above  $y_0$  in 1980. The magnitude and mix of the precursor emissions differ between air  
335 basins and transport of ozone between basins affects ambient ozone concentrations, so each basin  
336 has a characteristic value of  $A$ . The reductions in California anthropogenic emissions have  
337 driven a decrease in the magnitude of each basin's enhancement, which is well described as an  
338 exponential decrease with a time constant quantified by the parameter  $\tau = 21.9 \pm 1.2$  years. This  
339 value corresponds to a factor of 2 decrease in the ODV enhancement every  $15.2 \pm 0.8$  years for a  
340 total decrease of a factor of  $\sim 5$  from 1980 to 2015. Based on the analysis presented above, a  
341 similar value of  $\tau$  is found for all air basins, which may be reasonably expected since its  
342 magnitude reflects the history of emission controls, and these controls generally have been  
343 applied concurrently in all of the air basins. For example, vehicle emission control programs  
344 have been implemented simultaneously throughout California. While similar emission control  
345 programs may have had different effects in different air basins, such differences are not  
346 discernable in this analysis.

347 An important aspect of these results is the large magnitude derived for the U.S. background  
348 ODVs:  $62.0 \pm 1.9$  ppb in six of the air basins. The even larger value ( $75.6 \pm 2.5$  ppb) in the  
349 Salton Sea Air Basin will be discussed separately below. Two issues are important for  
350 understanding these high values. First, in the absence of enhancement of ozone from  
351 anthropogenic precursors, it is the very highest, i.e.  $\sim 98$ th percentile, of the U.S. background  
352 ozone concentrations that would be responsible for the ODVs. Second, baseline ozone  
353 transported ashore from the Pacific is the primary source of U.S. background ozone in  
354 California, and these baseline concentrations increase rapidly with altitude (Figure 1). Figure 6a  
355 compares the six basin U.S. background ODV determined here (i.e.,  $y_0$ ) with the altitude  
356 dependence of the 98<sup>th</sup> percentile of the baseline ozone concentrations measured at the surface

357 and by sondes at Trinidad Head, the northern California coastal site discussed earlier. The  
358 average of these highest baseline ozone concentrations in the 0 to 2 km altitude range are  
359 comparable to the basin  $y_0$  values derived in this analysis. We conclude that vertical mixing over  
360 California, and the altitude distribution of measurement sites within the air basins, may both  
361 contribute to the relatively large value of  $62.0 \pm 1.9$  ppb for the six basin U.S. background ODV  
362 derived here. These effects are discussed in more detail below. The impact of vertical mixing  
363 on surface air quality in northern California has been discussed previously (*Parrish et al.*, 2010).

364 Consideration of ODVs at specific sites can further clarify the magnitude of the U.S.  
365 background ODVs. With  $\tau$  set at 21.9 years, a fit of Equation 1 to the time series of ODVs at the  
366 Vandenberg Air Force Base site (see Figure S16 of the Supporting Information for details) gives  
367  $y_0 = 52.7 \pm 6.4$  ppb. This is the most isolated coastal site in southern California due to its  
368 location near sea level on the southwest corner of the South Central Coast Air Basin (location  
369 indicated in Figure 1), although pollution ozone from the Los Angeles urban area is occasionally  
370 transported to this site. The  $y_0$  at this site is significantly smaller than the U.S. background ODV  
371 for the basin ( $62.0 \pm 1.9$  ppb from Table 4), reflecting the site's low elevation, coastal location,  
372 which is where the smallest baseline ozone concentrations are expected. The surface site at  
373 Trinidad Head is a similarly isolated, near sea level coastal site in northern California that has  
374 been used to quantify baseline ozone concentrations (Figure 6a). ODVs have not been reported  
375 for this site, but the 98th percentile of the MDA8 ozone concentrations (i.e., approximately equal  
376 to the ODVs) during baseline conditions is 49 ppb, which is not statistically significantly  
377 different from the  $y_0$  value found for the Vandenberg Air Force Base site. Lassen Volcanic NP is  
378 a higher elevation (1.76 km) site in northern California that has also been used to quantify  
379 baseline ozone concentrations due to its relatively isolated location (*Jaffe et al.*, 2003; *Oltmans et*

380 *al.*, 2008; Parrish *et al.*, 2009; 2012). The U.S. background ODV derived at this site ( $68.5 \pm 9.0$   
381 ppb, Figure S17) is significantly larger than at Trinidad Head, and is not statistically significantly  
382 different from the  $62.0 \pm 1.9$  ppb found for the six southern California air basins.

383 The above comparison indicates that the U.S. background ODVs at sites in southern California  
384 air basins vary from about 50 ppb to 62 ppb (and even higher in the Salton Sea Air Basin). This  
385 variability is also clear in Figures S1-S8, which show the temporal evolution at a variety of sites  
386 within the eight air basins. This variability arises from variation in both the sources and sinks of  
387 U.S. background ozone. First, the vertical gradient in baseline ozone (Figures 1 and 6a)  
388 combined with the elevation distribution of the monitoring sites and with the varying influence  
389 of mixing larger ozone concentrations to the surface results in variations in baseline ozone  
390 transported to different sites. For example, the South Coast Air Basin contains all of the Los  
391 Angeles near-sea level urban sites, but also the rural Crestline site at an elevation of 1390 m.  
392 This latter site frequently records the largest ozone concentrations in the air basin, and because of  
393 its elevation may receive larger baseline ozone concentrations than lower elevation sites.  
394 Further, as air moves from the marine environment onto the continent, vertical mixing is  
395 enhanced, so the U.S. background ozone concentration at any particular surface location and  
396 time is affected by the average of the baseline ozone concentrations in all of the air parcels  
397 mixed to the surface. Vertical transport occurs through convection driven by solar heating of the  
398 land surface that causes the boundary layer to grow through entrainment of air from above.  
399 Winds interacting with the complex terrain of the California coast, where the coastal mountain  
400 ranges are in close proximity to the ocean, drive additional vertical mixing. The concentration of  
401 baseline ozone transported to a particular continental site is further modified by ozone loss to  
402 surfaces (particularly vegetation) and photochemical production from natural ozone precursors.

403 The net result is that surface U.S. background ozone concentrations are generally higher over the  
404 continent compared to coastal sea level sites; however the effects of vertical mixing and ozone  
405 production and loss processes vary significantly depending on site elevation, the character of the  
406 local and regional vertical mixing mechanisms, and the ozone loss and natural production  
407 processes, which are strong functions of the sites continental environment.

408 The time evolution of the ODVs in the Salton Sea and San Joaquin Valley air basins differs  
409 significantly from the other air basins. The reasons for these differences have not been  
410 established, but possible contributing factors can be mentioned. First, both the San Joaquin  
411 Valley and the Imperial Valley in the Salton Sea Air Basin are home to the most intensive  
412 agricultural activity in California; the State's emission control efforts have addressed emissions  
413 from the agricultural sector separately from emissions from other sectors such as mobile sources,  
414 electrical generation and industry. *Pusede and Cohen* (2012) emphasize the importance of a  
415 temperature dependent VOC source in the San Joaquin Valley that may be associated with  
416 agricultural emissions, and they argue that the region has or is transitioning to NO<sub>x</sub>-limited  
417 chemistry when temperatures are hottest and high ozone most probable. This transition may  
418 account for the different temporal evolution of the ODVs in the San Joaquin Valley Air Basin  
419 (Figures S7 and S14). Before the year 2000, little systematic change occurred in the ODVs, but  
420 from 2001-2015, the ODVs decreased at an exponential rate consistent with the other six air  
421 basins. A second contributing factor may help explain the larger  $y_0$  value ( $75.6 \pm 2.5$  ppb) in the  
422 Salton Sea Air Basin. That basin is adjacent to Mexico, and cross border transport of ozone or  
423 ozone precursors from emissions in Mexico, which are not subject to U.S. emission control  
424 efforts, may account for the elevated U.S. background ODV in that basin.

425 One complication in the identification of the parameter  $y_0$  as an estimate of the U.S.  
426 background ODV is that  $y_0$  is assumed constant in Equation 1; however systematic increases in  
427 baseline ozone concentrations at the North American west coast have been documented (*Jaffe et*  
428 *al.*, 2003; *Parrish et al.*, 2009; 2012; *Cooper et al.*, 2010). In order to investigate the impact of  
429 these changes in baseline ozone, we have updated the previous analysis of baseline ozone  
430 concentrations for near sea level, coastal sites along the North American west coast, primarily  
431 Trinidad Head California (*Parrish et al.*, 2009) and at the Lassen Volcanic NP site in the  
432 northern California mountains (*Parrish et al.*, 2012). The slowing and potential reversal of the  
433 increasing trend in seasonal average baseline ozone concentrations at these sites was quantified  
434 (*Parrish et al.*, 2012) by fitting 2nd order polynomials (e.g., curves in Figure 1) to the seasonal  
435 average data. The quadratic coefficients from the fits to the data then available (through 2010)  
436 were negative, indicating slowing of the increase, but were not statistically significant.  
437 Extension of the analysis through 2015 (manuscript in preparation, 2017) shows that with the  
438 five additional years of data included in the fits, the quadratic coefficients are indeed negative  
439 and statistically significant in all seasons, and that these coefficients agree (within their  
440 confidence limits) at the two sites. It is now clear that the increase in seasonal average baseline  
441 ozone concentrations discussed in previous work ended with maxima in the mid-2000s, and that  
442 the concentrations have begun to decrease in all seasons. The standard deviations of the seasonal  
443 baseline ozone concentrations over the complete data record vary from 2.3 to 3.6 ppb, which  
444 reflects both interannual variability (e.g., *Lin et al.*, 2015b) and the systematic trends. Compared  
445 to the change in ODVs discussed in this work, the systematic changes in baseline ozone  
446 concentrations are minor; thus, the assumption that the parameter  $y_0$  is constant is a good  
447 approximation.  $y_0$  should be interpreted as the average of the U.S. background ODV over the

448 1980 to 2015 period, with recognition that there have been small systematic changes in its  
449 magnitude.

450 One additional cautionary note should be considered in the physical interpretation of the  
451 parameter  $y_0$ . If there were a class of ozone precursor emissions not addressed by the emission  
452 control efforts implemented in California over the past decades, then ozone produced from these  
453 emissions would not have been reduced. Thus, this contribution to ambient ozone concentrations  
454 would serve to elevate  $y_0$  above the actual U.S. background ODV. However, since emission  
455 controls have been designed to reduce all known emission classes, it is unlikely that such a class  
456 of unknown ozone precursor emissions exists in all of the six air basins that exhibit a common  
457 value of  $y_0$ . Controls of agricultural emissions have not been implemented as extensively as for  
458 other anthropogenic emissions. The Imperial Valley in the Salton Sea Air Basin, the San  
459 Joaquin Valley, and the Salinas Valley in the North Coast Air Basin have intense agricultural  
460 activity, so  $y_0$  may be elevated above U.S. background ODVs in these basins, as discussed above  
461 for the San Joaquin Valley and Salton Sea Air Basins. Other basins have much less agricultural  
462 activity, so significant contributions from these emissions are not expected to generally raise all  
463  $y_0$  magnitudes,

464 **3.2. Shift of Seasonal Maximum Ozone Concentrations**

465 The physical interpretation of the derived parameters discussed in the preceding section has  
466 one implication that can be examined through ambient ozone concentration data. Baseline ozone  
467 transported into California, which is the primary source of U.S. background ozone, has a  
468 maximum in spring in the lower troposphere (e.g., *Oltmans et al.*, 2008), while local and regional  
469 ozone production from anthropogenic precursor emissions is expected to peak in the summer.  
470 Thus, as enhancement of ODVs from anthropogenic precursors has been reduced, we expect the

471 seasonal maximum in observed ozone concentrations to have shifted from summer toward  
472 spring. Figure 7 shows such a shift in all of the Southern California air basins. Data from the  
473 South Coast Air Basin are shown as an example in Figure 7a; here the dates of occurrence of the  
474 four highest MDA8 ozone concentrations are plotted. The color-coding indicates the decrease in  
475 ODV magnitude, and the slope of the linear regression to these data indicates that the seasonal  
476 maximum has moved to earlier in the year at an average rate of  $0.55 \pm 0.37$  day/year. When  
477 measurements were begun in the early 1970s, the seasonal maximum was on average in late July,  
478 and by 2015 it moved to early July. Figures S18 - S21 show similar plots for all eight air basins  
479 for both the four highest and the thirty highest MDA8 ozone concentrations recorded in each  
480 year; Figure 7b summarizes the results. Qualitatively similar shifts are found for all eight air  
481 basins, without significant differences between the four and thirty highest analyses.  
482 Quantitatively, the seasonal shift varies from near zero to approximately one day per year;  
483 further investigation is required to account for these differences between air basins. The near  
484 lack of a seasonal shift in the South Central Coast Basin is of particular interest.

485 The dates of the seasonal ozone maximum can be compared across the air basins by focusing  
486 on a particular year. Figure 7c shows the year 2000 intercept of the linear regressions in Figures  
487 S18 - S21. Here the four coastal air basins are shown on the left in light blue symbols, the two  
488 desert basins in orange symbols on the right, with the two other basins in between. The four  
489 coastal air basins all have maxima from mid to late July. The latest seasonal maximum is found  
490 in early August in the San Joaquin Valley Air Basin, with the earliest maxima in early July in the  
491 Salton Sea and the two desert air basins. These systematic differences in the seasonal maxima  
492 between air basins may provide useful metrics for investigating the performance of  
493 photochemical grid models of ozone formation in southern California. It is likely that models

494 must correctly reproduce the relative contributions of ozone from different sources to correctly  
495 reproduce these different seasonal cycles and their shifts in the different air basins. One  
496 particularly useful comparison may be the seasonal ozone maxima in the Mojave Desert and  
497 South Coast air basins. The former is very sparsely populated, so local photochemical  
498 production is expected to be quite limited, yet this basin exhibits large anthropogenic  
499 enhancements of ozone (see  $A$  value in Tables 1-4). These enhancements are believed to reflect  
500 transport of ozone from other air basins, primarily the South Coast and secondarily the San  
501 Joaquin Valley (e.g., *VanCuren*, 2015), yet the seasonal maximum occurs in the Mojave Desert  
502 well before those in these two source air basins. *Neuman et al.* (2012) noted this same difference  
503 in the ozone seasonality comparing Redlands (a site in the eastern South Coast Air Basin) with  
504 Joshua Tree NP (a site in the Mojave Desert Air Basin).

505 Similar shifts in the ozone seasonal cycle have been discussed previously. *Parrish et al.*  
506 [2013] show that the observed seasonal ozone maximum has shifted to earlier in the year over  
507 remote northern mid-latitudes during past decades. The sites considered in this work are  
508 primarily in Europe, but did include the Lassen NP site in northern California discussed above.  
509 The reported rates of change at these remote sites (3 to 6 days per decade) are similar to the rates  
510 shown in Figure 6b. However, the greater importance of background ozone at the more remote  
511 sites is reflected in the seasonal maxima occurring earlier in the summer than in southern  
512 California, generally mid to late June at sites outside of the MBL. A recent modeling study  
513 (*Clifton et al.*, 2014) suggests that the ozone seasonal maximum will continue to shift so that the  
514 seasonal cycle reverses (to a winter maximum) by late in the 21st century, at least in the  
515 northeast and the intermountain west regions of the U.S., although this work suggests that  
516 climate change as well as anthropogenic ozone emission reductions cause this shift.

517    **3.3. Projection of Future Basin ODVs and Relation to NAAQS**

518    In 2015 the basin ODVs in most of southern California exceeded the current NAAQS of 70  
519    ppb, in some cases by wide margins. Here we address an important policy-relevant question:  
520    How long will be required to reach the NAAQS in the southern California air basins? Equation  
521    1 provides an approximate answer to this question providing two key assumptions are valid:  
522    U.S. background ODV remains constant, and local emissions control strategies can continue the  
523    exponential decrease of the anthropogenic ozone enhancements into the future. The South Coast  
524    Air Basin had the highest basin ODV in 2015, so our initial focus is here. The reduction of  
525    ODVs in this basin over the past 35 years has been substantial - from 273 ppb in 1980 to 102 ppb  
526    in 2015 corresponding to a decrease of 171 ppb. A further reduction of 32 ppb (about 19% of the  
527    past reduction) will lower the ODV to the NAAQS. If the average absolute rate of decrease over  
528    the past 35 years (4.9 ppb/year) were to continue into the future, the NAAQS would be reached  
529    in seven years, or by 2022. However, projecting the past exponential decrease with the  
530    parameters from Table 4 suggests that a substantially longer time will be required. The ODV  
531    elevation above the U.S. background ODV (i.e.,  $y_0 = 62$  ppb) has been reduced from 211 ppb in  
532    1980 to 40 ppb in 2015, amounting to a factor of ~5 reduction. Reducing the remaining 40 ppb  
533    ODV elevation to the 8 ppb elevation necessary to reach the NAAQS will require a further factor  
534    of 5 reduction, which is projected to require an additional 35 years of control efforts, i.e. until  
535    2050. Figure 8 illustrates this projection for the South Coast and similar projections for the other  
536    six southern California air basins. The annotations in the figure indicate the year that the ODV  
537    in each basin will drop to the NAAQS. The projected ODV in one basin is already at or near 70  
538    ppb, but the projected years in five other basins are between 2030 and 2050. Since  $y_0$  in the  
539    Salton Sea Air Basin is greater than 70 ppb, this basin is projected to never reach the NAAQS; to

540 change this projection will require an understanding of why  $y_0$  is so high and strategies to reduce  
541 its magnitude. The 95 percent confidence limits on these projected years, based solely on the  
542 confidence limits of the parameters of Equation 1, vary from 1 year in the North Central Coast  
543 Air Basin to 5 years in the South Coast Air Basin.

544 Equation 1 gives precise projections for the future evolution of air basin ODVs, but the true  
545 uncertainty of future projections are undoubtedly larger than indicated by the above confidence  
546 limits. Even though Equation 1 provides an excellent description of past changes, there is no  
547 guarantee that future evolution will necessarily follow the same functional form. Still, since  
548 Equation 1 accurately fits 35 years of past ODV evolution, the projections do provide a useful  
549 guide for further thought., It should also be noted that detailed analyses of the temporal evolution  
550 of ambient concentrations of primary and secondary pollutants in the South Coast Air Basin  
551 demonstrate that many species, including VOCs, CO, NO<sub>x</sub>, HNO<sub>3</sub>, PAN, SO<sub>2</sub>, and PM<sub>2.5</sub>  
552 (Warneke *et al.*, 2012; Pollack *et al.*, 2013; Parrish *et al.*, 2016a) as well as ozone follow  
553 approximately exponential behavior. Evidently, the continuous efforts to reduce emissions  
554 maintained over multi-decadal time scales in southern California have yielded approximately  
555 exponential decreases.

556 **3.4 Comparison of derived parameters with model results**

557 An ideal model able to fully and accurately quantify the ozone budget in southern California  
558 would be able to reproduce the temporal evolution of the ODVs in each of the eight air basins  
559 considered in this work. The ten derived parameters included in Table 4 can serve as metrics to  
560 judge the performance of any model attempting to approach this ideal. To our knowledge, no  
561 modeling effort has attempted to reproduce the 36 years of ODV evolution considered here, so  
562 such a comprehensive evaluation is not yet possible. However, model studies have quantified

563 U.S. background ODVs, or closely related quantities, for southern California air basins; our goal  
564 here is to provide a brief, preliminary comparison of our U.S. background ODVs derived from  
565 observations with model results reported in the literature, and to discuss why disagreement may  
566 be expected.

567 Prior to this work, model calculations have provided the only means to estimate U.S.  
568 background ozone concentrations. In setting the new NAAQS, the U.S. EPA relied upon two  
569 different regional air quality models to estimate U.S. background ozone concentrations  
570 throughout the nation (*U.S. EPA*, 2015; *Dolwick et al.*, 2015). However, both of those regional  
571 models relied upon the GEOS-Chem global model to define the boundary conditions, i.e. the  
572 ozone concentrations entering the regional model domains. Another global model has calculated  
573 baseline ozone concentrations higher than those from GEOS-Chem (*Fiore et al.*, 2014), so a  
574 concern remains that the boundary conditions provided by GEOS-Chem may underestimate the  
575 ozone transported into the model domain. Thus, the regional air quality models in turn may have  
576 underestimated the U.S. background ozone concentrations, so that achieving the NAAQS may be  
577 more difficult than currently expected in some regions of the U.S. These issues emphasize the  
578 need for more rigorous evaluation of the global models that are used to provide the boundary  
579 conditions for regulatory ozone modeling.

580 Comparison of our observationally derived U.S. background ODVs with model results is  
581 somewhat ambiguous because most reported model results are based upon definitions of  
582 background ozone that differ from the U.S. background ODVs that we report in this work, and  
583 specific results are not generally reported for the southern California air basins considered in this  
584 work. Section S1 of the Supporting Information discusses how we interpreted the reported  
585 model results to arrive at the corresponding U.S. background ODVs we consider here.

586 The model results included in Figure 6b exhibit large variability, but taken as a whole are  
587 smaller than the U.S. background ozone ODVs estimated in this work; this difference suggests  
588 that the actual contribution of U.S. background ozone in southern California air basins may be  
589 larger than currently indicated by most model calculations. In contrast, one modeling study did  
590 give much higher estimates of U.S. background ODVs.

591 In addition to the large variability in the model results in Figure 6b, there are two additional  
592 reasons to question the reliability of model results designed to define U.S. background ozone  
593 concentrations. First, many models have unexplained systematic biases in the magnitude of  
594 calculated ozone concentrations compared to observations. *Dolwick et al.* (2015) use  
595 comparisons of model results to observations in an attempt to reduce the influence of such a bias,  
596 and *Fiore et al.* (2014) discuss a significant positive bias in the AM3 model total ozone  
597 concentration results (see their Figure 6). *Lin et al.* (2012), using a closely related AM3 model,  
598 were forced to correct for a related bias issue in the result included here in Figure 6b.

599 A second reason to question the accuracy of model derived ozone background concentrations  
600 is that quantitative comparisons of some global models with metrics derived from observations at  
601 baseline representative sites find substantial disagreements between models and measurements,  
602 and between different models (*Parrish et al.*, 2014; 2016b; *Derwent et al.*, 2016). These  
603 disagreements include significant model biases in absolute ozone concentrations, poor  
604 reproduction of ozone concentration changes over multi-decadal time periods, poor reproduction  
605 of ozone seasonal cycles within the MBL, and lack of adequate isolation of the MBL, at least at  
606 the U.S. west coast. For example, *Derwent et al.* (2016) compare results from fifteen global  
607 models with observations at the Trinidad Head surface site discussed in this paper; all models  
608 overestimated the observed annual mean ozone concentration of 31 ppb by 2 to 19 ppb, and the

609 observed amplitude of the fundamental of the seasonal cycle ( $5.7 \pm 0.9$  ppb) was poorly  
610 reproduced, with models giving amplitudes from 1.2 to 10.5 ppb. Difficulties in reproducing the  
611 ozone seasonal cycle over the U.S. are apparent in the one study cited here that compared two  
612 independent global models (*Fiore et al.*, 2014); one model simulated a large seasonal decline in  
613 mean NAB concentrations from springtime into summer, while the other found little seasonality.  
614 These comparisons suggest that global model results currently reported in the literature have  
615 substantial shortcomings that prevent their consistent and quantitatively accurate reproduction of  
616 important aspects of the global ozone distribution, and it is this distribution that determines U.S.  
617 background ozone.

618 In this work we have emphasized that vertical mixing over continental sites and its interaction  
619 with the strong vertical gradient of baseline ozone concentrations transported into California are  
620 important for determining U.S. background ozone concentrations. *Parrish et al.* (2016b) found  
621 that the treatment of the MBL dynamics in the three chemistry-climate models they considered  
622 was not adequate to reproduce the isolation of the MBL indicated by the observations at Trinidad  
623 Head. *Angevine et al.* (2012) demonstrate that mesoscale meteorological models have a difficult  
624 time accurately reproducing boundary layer heights and vertical mixing in California. Thus, to  
625 improve model calculations of U.S. background ozone concentrations in southern California, it  
626 may be useful to pay particular attention to the treatment of the vertical structure and transport in  
627 the lower troposphere.

628 **4. Conclusions and Recommendations**

629 The ozone NAAQS is based on a metric called the "ozone design value" (ODV); it is defined  
630 as the 3-year running mean of each year's 4th highest maximum daily 8-hour average (MDA8)  
631 ozone concentration measured at a monitoring site. To achieve compliance, the ODV must not

632 exceed the NAAQS, currently set at 70 ppb. We have investigated a set of ODVs for the eight  
633 air basins in southern California (Figure 1); each basin ODV is equal to the highest ODV  
634 calculated for any of the sites in the basin. These basin ODVs span the 36-year 1980-2015  
635 period, and in response to air quality improvement efforts, show strong systematic temporal  
636 decreases, although the 2015 ODVs still exceed the NAAQS in most of these air basins, some by  
637 wide margins. The temporal evolution of these ODVs has been investigated through several  
638 related approaches, and the results are summarized in Figures 2-5 and Tables 1-4. These  
639 approaches all show that a simple mathematical function (Equation 1) provides an excellent  
640 description of the temporal evolution of the ODVs. Figure 5 shows that 98.4% of the variability  
641 in a set of 214 ODV values from seven of the air basins is captured by Equation 1 with a total of  
642 10 parameter values, which are given in Table 4. Only three parameters of these parameters are  
643 required to define the temporal variability of the ODVs in all basins, with the other seven  
644 required to define the differences in the relative magnitudes of the ODVs between the air basins.

645 The parameter values in Table 4 are interpreted as providing estimates of physically significant  
646 quantities. The parameter  $y_0$  provides a quantification of the lower limit of the basin ODVs,  
647 toward which the measured ODVs are approaching. The value of  $y_0$  for an air basin is then an  
648 estimate of the lowest NAAQS that could possibly be achieved in that basin by reducing U.S.  
649 anthropogenic ozone precursor emissions to zero, leaving only  $y_0$ , which we call the U.S.  
650 background ODV. However, as seen in the Salton Sea Air Basin,  $y_0$  may be elevated above the  
651 true U.S. background ODV if there are impacts from a heretofore uncontrolled or less controlled  
652 emissions sector, such as agriculture. It follows that the parameter  $A$  is then interpreted as the  
653 enhancement of the basin ODV above  $y_0$  in 1980, and that  $\tau$  is the time constant for the  
654 exponential decrease of this ODV enhancement. A single value of  $\tau = 21.9 \pm 1.2$  years fits all

655 seven air basins; this value indicates that a factor of 2 decrease in the basin ODV enhancements  
656 occurred every  $15.2 \pm 0.8$  years for a total decrease of a factor of  $\sim 5$  from 1980 to 2015. A  
657 single value of  $y_0 = 62.0 \pm 1.9$  ppb fit six air basins, with a significantly higher value ( $75.6 \pm 2.5$   
658 ppb) required for the Salton Sea air basin. A different value of  $A$  is found for each air basin. The  
659 1.6% of the variability not captured with the 10-parameter fit to Equation 1 is primarily due to  
660 interannual variability about the fit, so that it has not been possible to further differentiate  
661 between the common values of  $y_0$  and  $\tau$  derived for these seven air basins. The U.S. background  
662 ODVs derived here are larger than generally appreciated; their large magnitudes emphasize the  
663 importance of vertical mixing bringing higher ozone concentrations to the surface from aloft, as  
664 emphasized by the results in Figure 6a.

665 Two implications of the derived description of the temporal evolution of the basin ODVs are  
666 investigated. First, a change in the seasonal cycle of ozone in southern California over the 1980-  
667 2015 period is expected, as the predominant contribution to observed ozone concentrations  
668 shifted from photochemical production driven by anthropogenic precursors (with a summer  
669 maximum) to predominately the U.S. background contribution (with a spring maximum). Figure  
670 7 shows that the seasonal cycle of ozone has indeed shifted to earlier in the year in all eight air  
671 basins in accord with this expectation; the rate of this shift has varied from near zero to  $\sim 1$   
672 day/year. Second, Equation 1 provides the basis for a projection of future evolution of the basin  
673 ODVs illustrated in Figure 8. This projections depends on two key assumptions: emission  
674 control efforts can maintain the past exponential decrease of the anthropogenic ozone  
675 enhancements with the same value of  $\tau$ , and the U.S. background ODV ( $y_0$ ) remains constant.  
676 The resulting projection is rather pessimistic. For example, over the 1980 to 2015 data record,  
677 the ODV enhancement above  $y_0$  in the South Coast Air basin decreased markedly - from 211 ppb

678 in 1980 to 40 ppb in 2015 (a factor of ~5 reduction); however, reducing the remaining 40 ppb  
679 ODV enhancement to the 8 ppb enhancement necessary to reach the 70 ppb NAAQS requires a  
680 further factor of 5 reduction, which is projected to require an additional 35 years of control  
681 efforts, i.e. until 2050. The other air basins with smaller anthropogenic ozone enhancements are  
682 projected to reach the NAAQS in earlier years as illustrated in Figure 8.

683 Some features of the basin ODVs and their temporal evolution remain unexplained;  
684 investigating the causes of these features may provide fruitful foci for future research.

- 685 • The derived value of  $y_0$  for the Salton Sea air basin is significantly larger ( $75.6 \pm 2.3$   
686 ppb) than for the other air basins ( $62.0 \pm 1.9$  ppb). The influence of agricultural  
687 emissions and transport of precursors and/or ozone from Mexico are suggested as  
688 possible causes.
- 689 • The temporal decrease of the ODVs for the San Joaquin Air Basin was quite slow before  
690 the year 2000, but since that year the decrease has proceeded at a rate similar to the other  
691 air basins. The influence of agricultural emissions is again suggested as a cause.
- 692 • The rate of the shift in the ozone seasonal cycle and the timing of the seasonal maximum  
693 differ significantly between basins; these differences are not understood.

694 A brief, preliminary comparison of the U.S. background ODVs derived here from observations  
695 with results from models reported in the literature is given in Section 3.4 and Figure 6b. For the  
696 most part, there are not large differences, although most models seem to give smaller estimates;  
697 in contrast *Mueller and Mallard* (2011) calculated significantly larger North American  
698 background ODVs. In addition, comparisons of calculations by several global models with  
699 measured ambient concentrations at Trinidad Head, a baseline site on the northern California  
700 coast, found poor agreement with absolute ozone concentrations, the ozone seasonal cycle, and

701 the isolation of the MBL (*Parrish et al.*, 2014; 2016b; *Derwent et al.*, 2016). These comparisons  
702 suggest that the ability of current modeling systems to provide consistent and accurate  
703 calculations of U.S. background ozone concentrations is limited.

704 It may be possible to significantly advance modeling systems in order to improve our  
705 understanding of U.S. and North American background ozone concentrations in southern  
706 California's air basins. Equation 1 with the parameter values listed in Table 4 provides an  
707 excellent description of the temporal evolution of southern California's air basins. Analogous  
708 parameter values can be extracted from model calculations designed to reproduce this temporal  
709 evolution, and these derived parameters can be compared to those in Table 4, which would serve  
710 as comparison metrics. The characterization of the ozone seasonal cycle in Section 3.2 gives the  
711 parameters illustrated in Figure 7, which constitute additional comparison metrics. The  
712 comparisons of global model results with measurements at Trinidad Head, CA provide further  
713 metrics for comparison (*Parrish et al.*, 2014; 2016b; *Derwent et al.*, 2016). A concerted,  
714 systematic effort to improve current modeling systems, so that accurate reproduction of all of  
715 these metrics is improved, may yield an improved tool for quantifying U.S. background ozone  
716 concentrations and the temporal evolution of observed ambient ozone concentrations, at least in  
717 California and perhaps other regions of the country.

718 **Acknowledgments**

719 The authors acknowledge support from NOAA's Health of the Atmosphere and Atmospheric  
720 Chemistry and Climate Programs. The CareerLaunch Internship Program of Denver Public  
721 Schools supported LMY. The STAR (STEM Teacher and Researcher) Program of California  
722 State University supported MHN. The California Air Resources Board provided maximum 8-hr  
723 ozone concentrations. Ozone design values were calculated by the California Air Resources

724 Board and downloaded from: <http://www.arb.ca.gov/adam/index.html>. NOAA Earth System  
725 Research Laboratory, Global Monitoring Division provided surface and ozone sonde data from  
726 Trinidad Head (McClure-Begley, A., Petropavlovskikh, I., Oltmans, S., (2014) NOAA Global  
727 Monitoring Surface Ozone Network. 2012-2014: National Oceanic and Atmospheric  
728 Administration, Earth Systems Research Laboratory Global Monitoring Division. Boulder,  
729 CO. <http://dx.doi.org/10.7289/V57P8WBF>). The National Park Service provided ozone data  
730 from Lassen NP. The authors are grateful to Owen R. Cooper and Andrew O. Langford for  
731 extensive, helpful discussions. Disclosure: David Parrish also works as an atmospheric  
732 chemistry consultant ([David D. Parrish, LLC](#)); he has had contracts funded by several state and  
733 federal agencies, although they did not support this work.

734 **References**

- 735 Angevine, W. M., L. Eddington, K. Durkee, C. Fairall, L. Bianco, and J. Brioude (2012),  
736 Meteorological model evaluation for CalNex 2010, *Mon. Weather Rev.*, 140, 3885–3906,  
737 doi:10.1175/MWR-D-12-00042.1.
- 738 Ayers, G.P., et al. (1992), Evidence for photochemical control of ozone concentrations in  
739 unpolluted marine air, *Nature*, 360, 446-449.
- 740 Bevington, P.R., and D.K. Robinson (2003), Data reduction and error analysis for the physical  
741 sciences, 3rd edition, McGraw-Hill, New York, N.Y.
- 742 Clifton, O. E., A. M. Fiore, G. Correa, L. W. Horowitz, and V. Naik (2014), Twenty-first century  
743 reversal of the surface ozone seasonal cycle over the northeastern United States, *Geophys.  
744 Res. Lett.*, 41, 7343–7350, doi:10.1002/ 2014GL061378.
- 745 Cooper, O. R., et al. (2010), Increasing springtime ozone mixing ratios in the free troposphere  
746 over western North America, *Nature*, 463, 344-348.
- 747 Cooper, O.R., A.O. Langford, D.D. Parrish, and D.W. Fahey (2015), Challenges of a lowered  
748 U.S. ozone standard, *Science*, 348(6239), 1096-1097, doi:10.1126/science.aaa5748.
- 749 Derwent, R. G., D. D. Parrish, I. E. Galbally, D. S. Stevenson, R. M. Doherty, P. J. Young, and  
750 D. E. Shallcross (2016), Interhemispheric differences in seasonal cycles of tropospheric

- 751 ozone in the marine boundary layer: Observation-model comparisons, *J. Geophys. Res.*  
752 *Atmos.*, 121, doi:10.1002/2016JD024836.
- 753 Dolwick, P., et al., (2015) Comparison of background ozone estimates over the western United  
754 States based on two separate model methodologies, *Atmos. Environ.*, 109, 282-296.
- 755 Emery, C., et al. (2012), Regional and global modeling estimates of policy relevant background  
756 ozone over the United States, *Atmos. Environ.*, 47, 206-217.
- 757 Fiore, A.M., et al., (2014) Estimating North American background ozone in U.S. surface air with  
758 two independent global models: Variability, uncertainties, and recommendations, *Atmos.*  
759 *Environ.* 96, 284-300.
- 760 Jaffe, D., H. Price, D.D. Parrish, A. Goldstein, and J. Harris (2003), Increasing background  
761 ozone during spring on the west coast of North America, *Geophys. Res. Lett.*, 30 (12), 1613,  
762 doi:10.1029/2003GL017024.
- 763 Lefohn, A.S., et al., (2014) Estimates of background surface ozone concentrations in the United  
764 States based on model-derived source apportionment, *Atmos. Environ.*, 84, 275-288.
- 765 Lin, M., A. M. Fiore, O. R. Cooper, L. W. Horowitz, A. O. Langford, H. Levy II, B. J. Johnson,  
766 V. Naik, S. J. Oltmans, and C. J. Senff (2012), Springtime high surface ozone events over the  
767 western United States: Quantifying the role of stratospheric intrusions, *J. Geophys. Res.*, 117,  
768 D00V22, doi:10.1029/2012JD018151.
- 769 Lin, M., L. W. Horowitz, O. R. Cooper, D. Tarasick, S. Conley, L. T. Iraci, B. Johnson, T.  
770 Leblanc, I. Petropavlovskikh, and E. L. Yates (2015a), Revisiting the evidence of increasing  
771 springtime ozone mixing ratios in the free troposphere over western North America,  
772 *Geophys. Res. Lett.*, 42, 8719–8728, doi:10.1002/2015GL065311.
- 773 Lin, M. Y., A. M. Fiore, L. W. Horowitz, A. O. Langford, S. J. Oltmans, D. Tarasick, and H. E.  
774 Rieder (2015b), Climate variability modulates western U.S. ozone air quality in spring via  
775 deep stratospheric intrusions, *Nature Communications*, 6(7105), doi:10.1038/ncomms8105.
- 776 Mueller, S.F., Mallard, J.W., 2011. Contributions of natural emissions to ozone and PM<sub>2.5</sub> as  
777 simulated by the community multiscale air quality (CMAQ) model. *Environ. Sci. Technol.*  
778 45, 4817e4823.
- 779 Neuman, J. A., et al. (2012), Observations of ozone transport from the free troposphere to the  
780 Los Angeles basin, *J. Geophys. Res.*, 117, D00V09, doi:10.1029/2011JD016919.
- 781 Oltmans, S.J., et al. (2008), Background ozone levels of air entering the west coast of the US and  
782 assessment of longer-term changes, *Atmos. Environ.*, 42 6020-6038.

- 783 Oltmans, S.J., and H. Levy II (1992), Seasonal cycle of surface ozone over the western North  
784 Atlantic, *Nature* 358, 392-394.
- 785 Oltmans, S.J., and H. Levy II (1994), Surface ozone measurements from a global network,  
786 *Atmos. Environ.*, 28, 9-24.
- 787 Parrish, D.D., D.B. Millet, and A.H. Goldstein (2009), Increasing ozone in marine boundary  
788 layer air inflow at the west coasts of North America and Europe, *Atmos. Chem. Phys.*,  
789 9, 1303–1323.
- 790 Parrish, D.D., K.C. Aikin, S.J. Oltmans, B.J. Johnson, M. Ives, and C. Sweeny (2010), Impact of  
791 transported background ozone inflow on summertime air quality in a California ozone  
792 exceedance area, *Atmos. Chem. Phys.*, 10, 10093–10109, doi:10.5194/acp-10-10093-2010.
- 793 Parrish, D.D., K.S. Law, J. Staehelin, R. Derwent, O.R. Cooper, H. Tanimoto, A. Volz-Thomas,  
794 S. Gilge, H.-E. Scheel, M. Steinbacher and E. Chan (2012), Long-term changes in lower  
795 tropospheric baseline ozone concentrations at northern mid-latitudes, *Atmos. Chem. Phys.*,  
796 12, 11485–11504.
- 797 Parrish, D. D., K. S. Law, J. Staehelin, R. Derwent, O. R. Cooper, H. Tanimoto, A. Volz-  
798 Thomas, S. Gilge, H.-E. Scheel, M. Steinbacher, and E. Chan (2013), Lower tropospheric  
799 ozone at northern midlatitudes: Changing seasonal cycle, *Geophys. Res. Lett.*, 40, 1631–  
800 1636, doi: 10.1002/grl.50303.
- 801 Parrish, D.D., et al. (2014), Long-term changes in lower tropospheric baseline ozone  
802 concentrations: Comparing chemistry-climate models and observations at northern  
803 midlatitudes, *J. Geophys. Res. Atmos.*, 119, 5719–5736, doi:10.1002/2013JD021435.
- 804 Parrish, D.D., J. Xu, B. Croes and M. Shao, Air Quality Improvement in Los Angeles -  
805 Perspective for Developing Cities (2016a), *Frontiers of Environ Sci. & Engineering*, 10(5):  
806 11, Doi: 10.1007/s11783-016-0859-5
- 807 Parrish, D. D., et al. (2016b), Seasonal cycles of O<sub>3</sub> in the marine boundary layer: Observation  
808 and model simulation comparisons, *J. Geophys. Res. Atmos.*, 121, 538–557,  
809 doi:10.1002/2015JD024101.
- 810 Pfister, G. G., D. Parrish, H. Worden, L. K. Emmons, D. P. Edwards, C. Wiedinmyer, G. S.  
811 Diskin, G. Huey, S. J. Oltmans, V. Thouret, A. Weinheimer and A. Wisthaler (2011),  
812 Characterizing summertime chemical boundary conditions for airmasses entering the US  
813 West Coast, *Atmos. Chem. Phys.*, 11, 1769–1790, 2011, doi:10.5194/acp-11-1769-2011.
- 814 Pollack, I. B., T. B. Ryerson, M. Trainer, J. A. Neuman, J. M. Roberts, and D. D. Parrish (2013),  
815 Trends in ozone, its precursors, and related secondary oxidation products in Los Angeles,

- 816 California: A synthesis of measurements from 1960 to 2010, *J. Geophys. Res. Atmos.*, *118*,  
817 5893–5911, doi:10.1002/jgrd.50472.
- 818 Pusede, S.E., and R.C. Cohen (2012), On the observed response of ozone to NOX and VOC  
819 reactivity reductions in San Joaquin Valley California 1995–present, *Atmos. Chem. Phys.*, *12*,  
820 8323–8339, www.atmos-chem-phys.net/12/8323/2012/doi:10.5194/acp-12-8323-2012.
- 821 U.S. EPA (2015), "Implementation of the 2015 Primary Ozone NAAQS: Issues Associated with  
822 Background Ozone White Paper for Discussion"  
823 <https://www.epa.gov/sites/production/files/2016-03/documents/whitepaper-bgo3-final.pdf>,  
824 most recently accessed 11 November 2016.
- 825 VanCuren, R. (2015) Transport aloft drives peak ozone in the Mojave Desert, *Atmos. Environ.*,  
826 *109*, 331–341, dx.doi.org/10.1016/j.atmosenv.2014.09.057.
- 827 Wang, H., Jacob, D.J., Le Sager, P., Streets, D.G., Park, R.J., Gilliland, A.B., van Donkelaar, A.,  
828 2009. Surface ozone background in the United States: Canadian and Mexican pollution  
829 influences. *Atmospheric Environment* *43*, 1310e1319.
- 830 Warneke, C., J. A. de Gouw, J. S. Holloway, J. Peischl, T. B. Ryerson, E. Atlas, D. Blake, M.  
831 Trainer, and D. D. Parrish (2012), Multiyear trends in volatile organic compounds in Los  
832 Angeles, California: Five decades of decreasing emissions, *J. Geophys. Res.*, *117*, D00V17,  
833 doi:10.1029/2012JD017899.
- 834 Zhang, L., Jacob, D.J., Downey, N.V., Wood, D.A., Blewitt, D., Carouge, C.C., van Donkelaar,  
835 A., Jones, D.B.A., Murray, L.T., Wang, Y., 2011. Improved estimate of the policy-relevant  
836 background ozone in the United States using the GEOS-Chem global model with  $1/2^\circ \times 2/3^\circ$   
837 horizontal resolution over North America. *Atmospheric Environment*.  
838 doi:10.1016/j.atmosenv.2011.07.054.

839 **TABLES.**

840 **Table 1.** Time period of basin ozone design values included in analysis and results of least-  
 841 squares fits to Equation (1) with  $\tau$  set to 22.3 years. These parameters are from the least square  
 842 fits illustrated in Figure 2 and Figures S1-S6.

843

Air Basin	years	$y_0$ (ppb)	A (ppb)	$\sigma$ (ppbv)
South Coast	1980 - 2015	$58.9 \pm 7.0$	$204 \pm 13$	4.9
San Diego	1980 - 2015	$63.9 \pm 5.8$	$83 \pm 10$	4.1
South Central Coast	1980 - 2015 <sup>1</sup>	$62.9 \pm 6.6$	$94 \pm 12$	4.7
North Central Coast <sup>2</sup>	1989 - 2015	62.9	40	3.1
Mojave Desert	1987 - 2015	$58.4 \pm 7.7$	$145 \pm 17$	4.1
San Joaquin Valley	1980 - 2015	----	----	----
Salton Sea	1980 - 2015	$75.8 \pm 4.8$	$74 \pm 9$	3.4
Great Basin Valleys	1986 - 2015	----	----	----

844 <sup>1</sup> 1986 excluded from the fit as discussed in the text.

845 <sup>2</sup> The functional fit to the North Central Coast ODVs gives  $y_0 = 64.9 \pm 6.3$  and  $A = 24 \pm 15$ . The values in the  
 846 table are for  $y_0$  set equal to that of the South Central Coast as discussed in the text.

847  
848

849 **Table 2.** Results of evaluation of least-squares fits to Equation (1). These parameters are from  
 850 the linear regressions illustrated in Figure 3.

Air Basin	$\tau$ (years)	A (ppb)	$r^2$	$\sigma$ (%) <sup>2</sup>
South Coast	$22.2 \pm 1.3$	$204 \pm 11$	0.99	5
San Diego	$21.0 \pm 2.5$	$86 \pm 10$	0.96	10
South Central Coast	$19.8 \pm 2.5$	$101 \pm 13$	0.96	11
North Central Coast <sup>1</sup>	$20.6 \pm 8.2$	$43 \pm 20$	0.76	22
Mojave Desert	$23.0 \pm 3.2$	$139 \pm 19$	0.96	8
Salton Sea	$21.9 \pm 3.0$	$74 \pm 9$	0.95	11

851 <sup>1</sup> The values in the table are for  $y_0$  set equal to that of the South Central Coast as discussed in the text.

852 <sup>2</sup> The  $\sigma$  values give approximate relative root-mean-square deviation (in %), which are calculated from  
 853  $(\chi^2/(n-2))^{1/2}$ , where  $\chi^2$  is the sum of the squares of the deviations of the log-transformed data from the linear  
 854 fits in Figure 3, and n is the number of data points.

855  
856  
857  
858

859 **Table 3.** Results of correlation of air basin ODVs with those of the South Coast Air Basin.  
 860 These parameters are from the linear regressions illustrated in Figure 4 and Figures S9-S15.

Air Basin	$y_0$ (ppb)	$A$ (ppb)	$r^2$
South Coast	58.9	204	----
San Diego	$63.9 \pm 3.9$	$83 \pm 7$	0.96
South Central Coast	$62.8 \pm 4.0$	$94 \pm 7$	0.95
North Central Coast	$64.9 \pm 5.4$	$36 \pm 13$	0.73
Mojave Desert	$59.5 \pm 5.7$	$142 \pm 13$	0.98
San Joaquin Valley <sup>1</sup>	$61 \pm 18$	$(155 \pm 62)$	0.92
Salton Sea	$75.9 \pm 3.8$	$73 \pm 7$	0.96
Great Basin Valleys	----	----	0.38

861 <sup>1</sup> Only the years 2001-2015 are included in the fits to this air basin as discussed in the text.  
 862

863

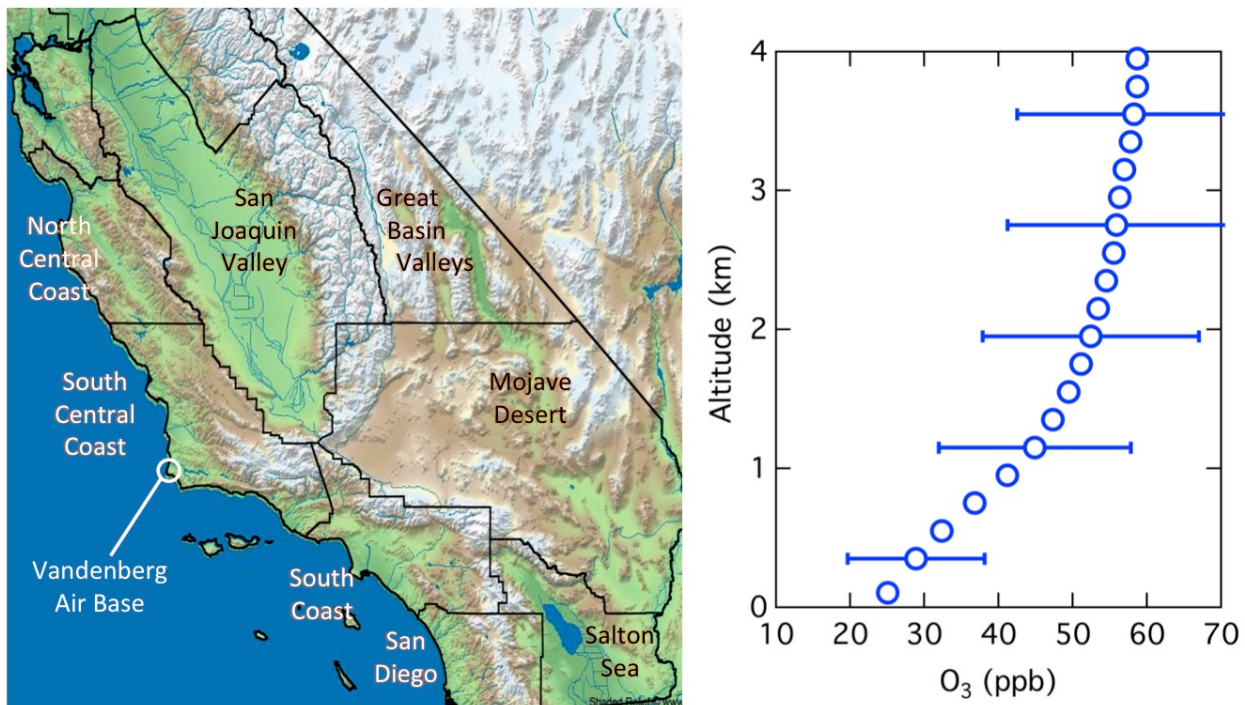
864

865 **Table 4.** Results of multivariate least-squares analysis illustrated in Figure 5. The ten parameters  
 866 extracted from that analysis are included, along with the absolute root-mean-square deviations  
 867 between the observed ODVs and the derived fits.

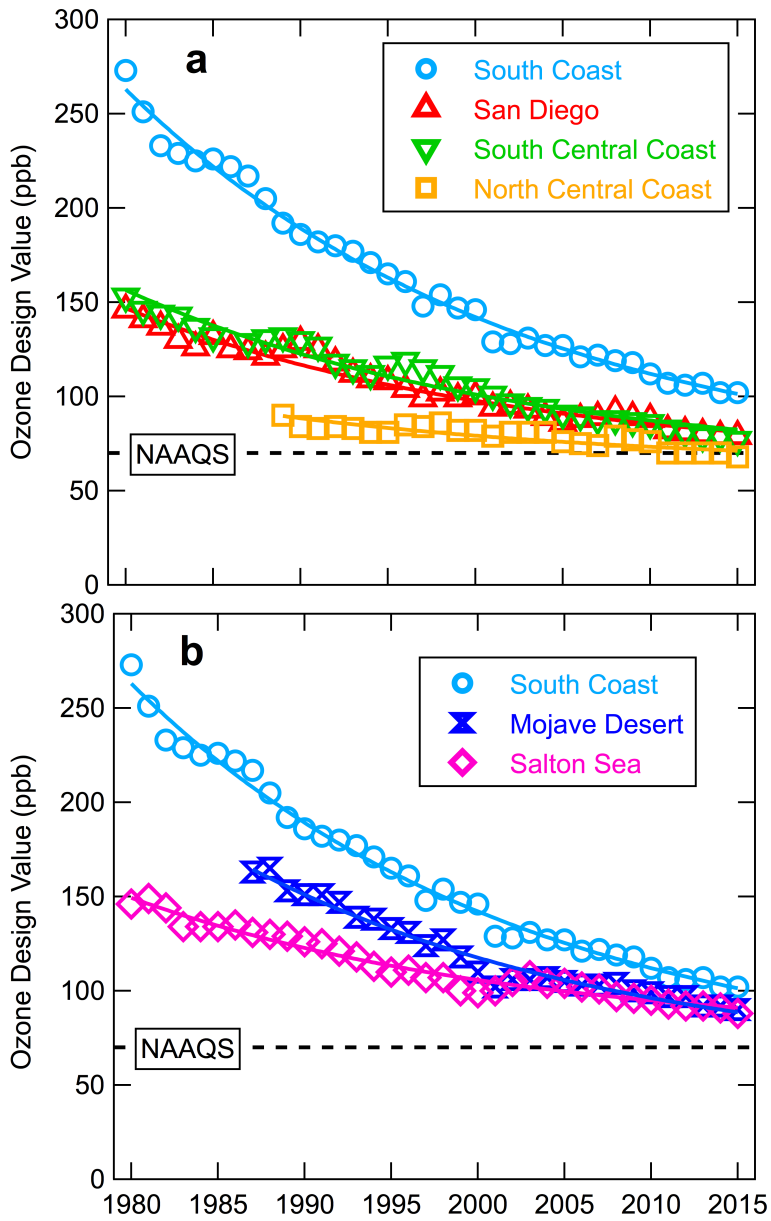
Air Basin	$\tau$ (years)	$y_0$ (ppb)	$A$ (ppb)	$\sigma$ (ppb)
South Coast	$21.9 \pm 1.2$	$62.0 \pm 1.9$	$197 \pm 8$	5.3
San Diego	<sup>2</sup>	<sup>2</sup>	$86 \pm 5$	4.2
South Central Coast	<sup>2</sup>	<sup>2</sup>	$95 \pm 5$	4.7
North Central Coast	<sup>2</sup>	<sup>2</sup>	$41 \pm 5$	3.1
Mojave Desert	<sup>2</sup>	<sup>2</sup>	$136 \pm 7$	4.3
San Joaquin Valley <sup>1</sup>	<sup>2</sup>	<sup>2</sup>	$(149 \pm 12)$	3.4
Salton Sea	<sup>2</sup>	$75.6 \pm 2.5$	$73 \pm 5$	3.6

868 <sup>1</sup> Only the years 2001-2015 are included in the fits to this air basin as discussed in the text.  
 869 <sup>2</sup> Value given for South Coast Air Basin applies to this air basin as well.  
 870

871 **FIGURES**

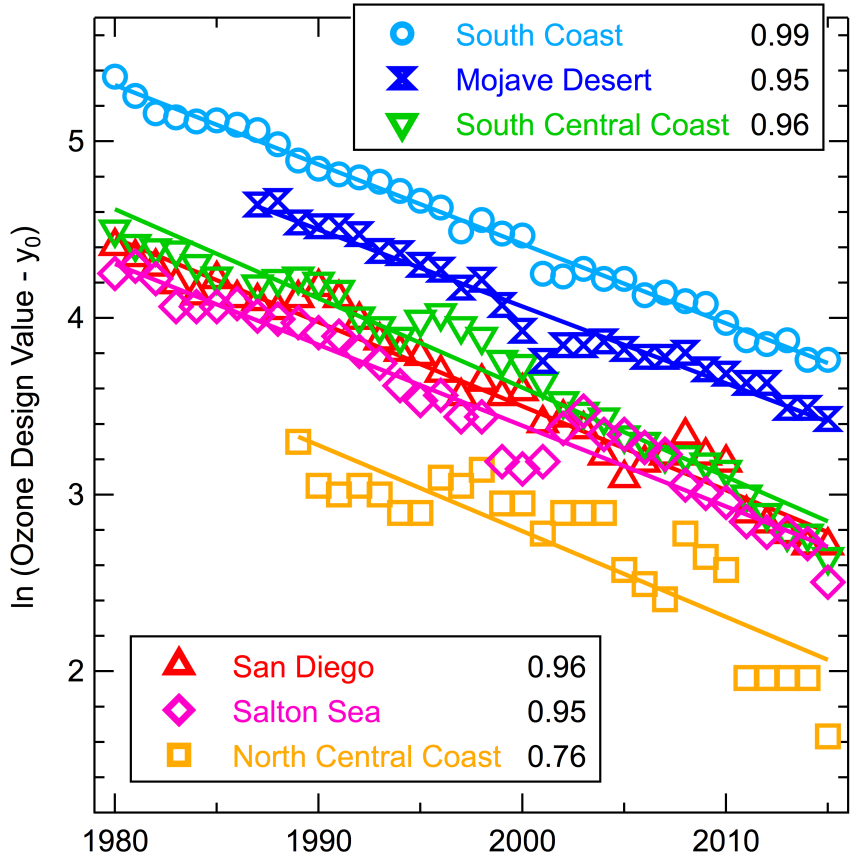


872  
873 **Figure 1.** Map of the eight southern California air basins and plot of the vertical profile of  
874 baseline ozone concentrations measured by 471 ozone sondes released at Trinidad Head, a  
875 northern California coastal site (*Oltmans et al., 2008*) during the 5-month (May-September)  
876 ozone season from 1997 through 2014.., The symbols show averages over 200 m altitude  
877 increments with error bars giving example standard deviations.  
878



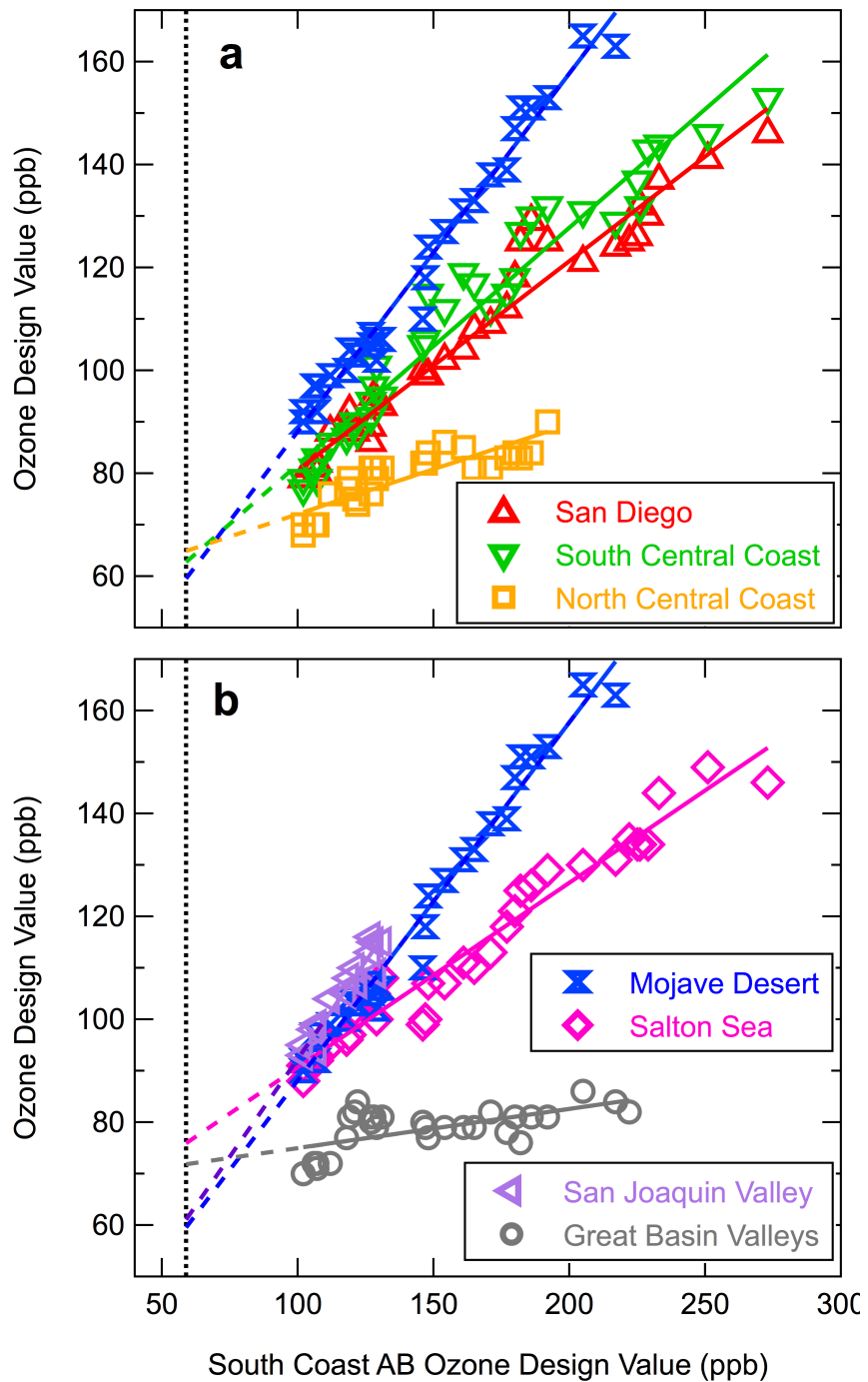
879

880 **Figure 2.** Evolution of the ozone design values over the past 36 years in **a)** the four southern  
 881 California coastal air basins and **b)** two inland air basins with the South Coast included for  
 882 comparison. The symbols give the annual ODVs for each air basin, and the solid curves indicate  
 883 the fits of Equation 1 to the corresponding ODVs. The dashed line indicates the 2015 NAAQS.



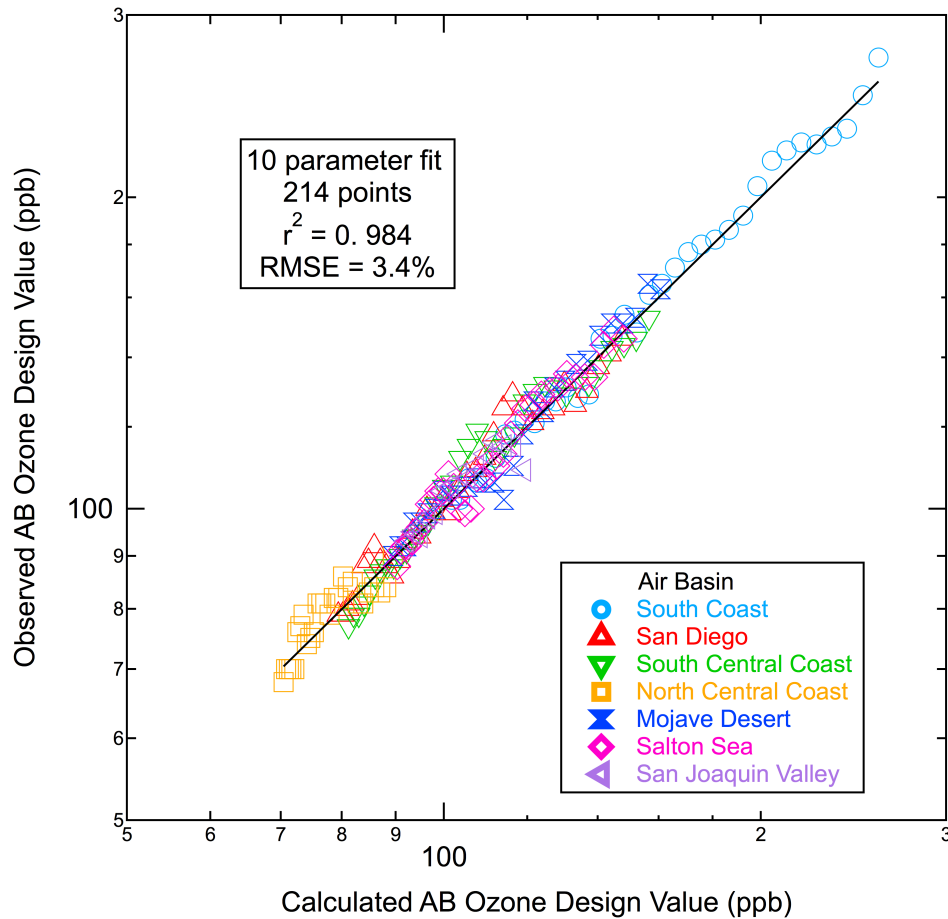
884

885 **Figure 3.** Evolution of the natural logarithm of the ODV enhancement above  $y_0$  over the past 36  
 886 years in six southern California air basins. The straight lines indicate linear regression fits to the  
 887 symbols, with the  $r^2$  of those fits indicated in the annotations.



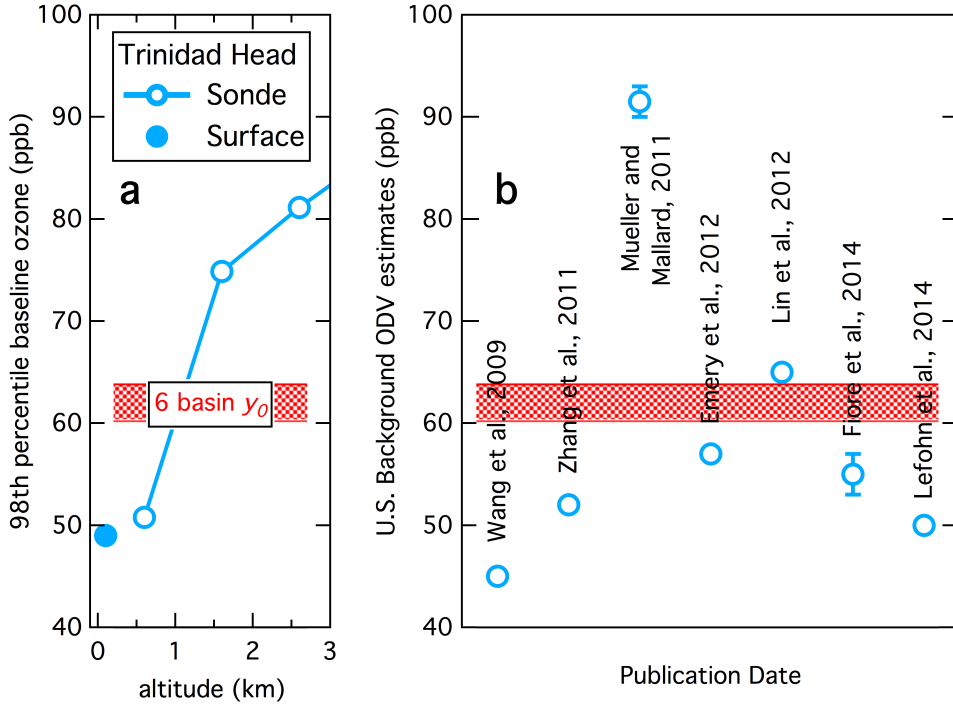
888

889 **Figure 4.** Correlations of ODVs between Southern California air basins and the South Coast Air  
 890 Basin. The solid lines indicate linear regressions to the symbols. The dashed lines are  
 891 extrapolations of the linear fits to the  $y_0$  value = 58.9 ppb determined for the South Coast Air  
 892 Basin (vertical dotted line).

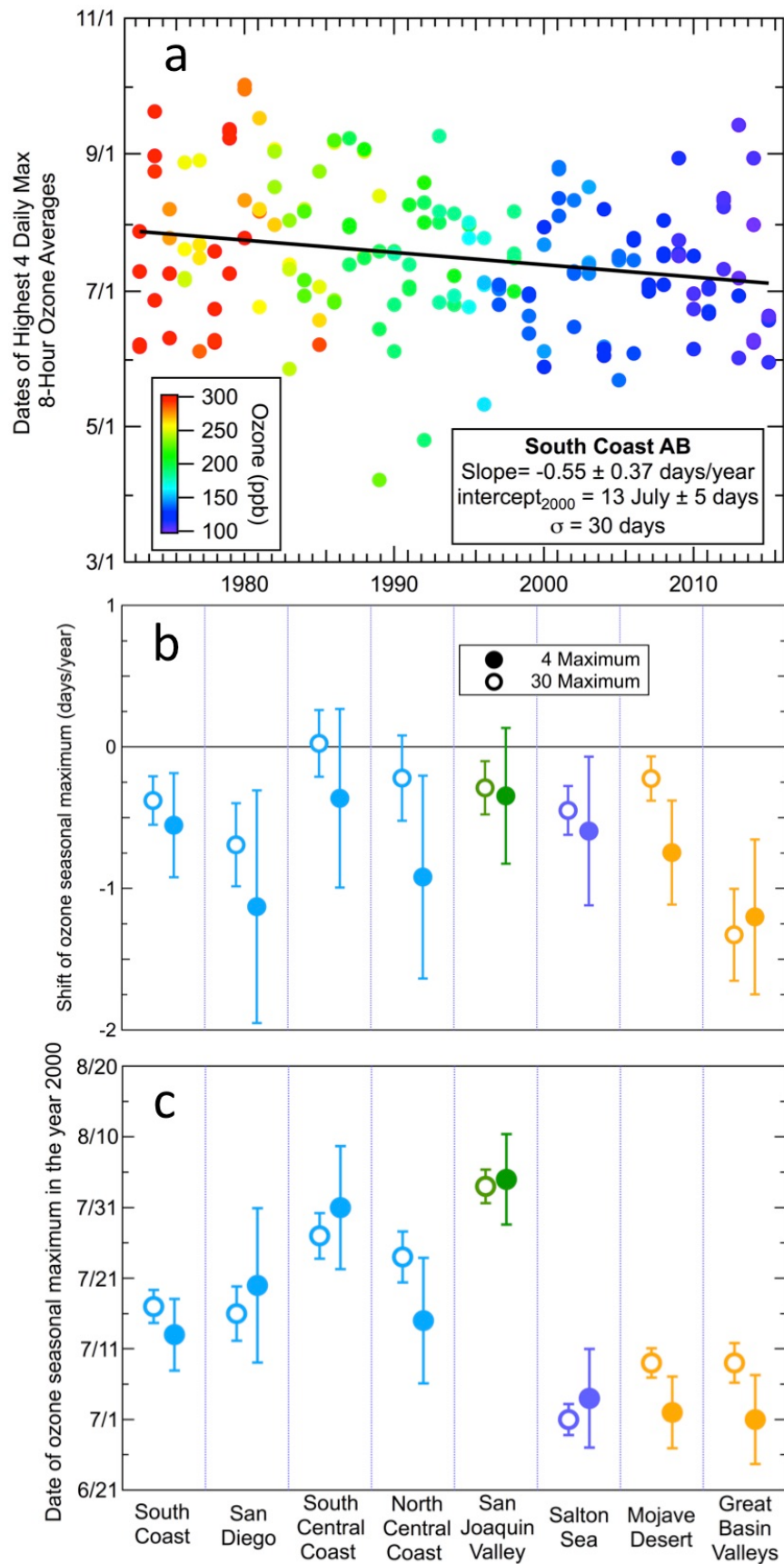


893

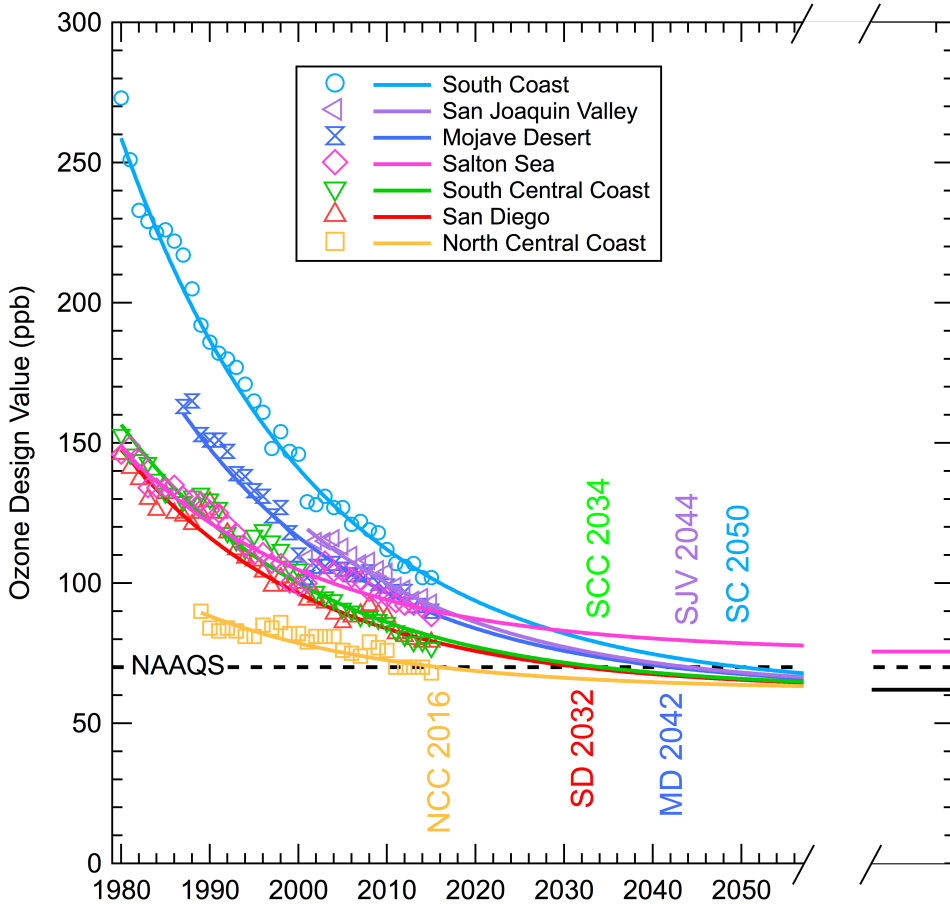
894 **Figure 5.** Comparison of observed ODVs with those calculated from Equation (1) based upon a  
 895 multivariate regression with ten parameters for seven air basins (Table 4). The solid line  
 896 indicates the 1:1 relationship. The total number of data points, the square of the correlation  
 897 coefficient for the log-transformed data, and the root-mean-square relative deviations of the  
 898 calculated ODVs are indicated.



899      **Figure 6.** Comparison of  $y_0$  determined for six air basins with **a)** the 98th percentile of the  
900      baseline ozone concentrations measured at Trinidad Head in May through September and **b)**  
901      estimates of the U.S. background ODV from modeling studies. The red hatched bar indicates the  
902      six basin  $y_0 \pm$  confidence limits in both plots. In **a)** the solid symbol gives the Trinidad Head  
903      surface result and the open symbols give the results from the sonde data (also included in Figure  
904      1) averaged over 1 km thick layers beginning at 0.1 km. The symbols in **b)** give the results from  
905      model calculations estimated from the indicated literature references; Section S1 of the  
906      Supplementary Information gives details of the interpretation of these model results.  
907



909     **Figure 7.** Evolution of the dates of occurrence of the highest maximum daily 8-hour average  
910     (MDA8) ozone concentrations over the past 42 years in the Southern California air basins. **a)**  
911     Symbols indicate the dates that the four highest maxima were recorded in the South Coast Air  
912     Basin each year, and are color-coded according to the ozone concentration. The solid line gives  
913     the linear regression fit to the symbols; slopes and intercepts with 95% confidence limits and the  
914     root mean square deviation from the fit are annotated. Comparison of **b)** rate of change of ozone  
915     seasonal maximum and **c)** the date of the seasonal maximum in the year 2000 in the eight  
916     southern California air basins. The results for the four (closed symbols) and the thirty (open  
917     symbols) highest MDA8 concentrations in each year are shown with 95% confidence limits.  
918



919

920 **Figure 8.** Past and projected evolution of the basin ozone design values in seven southern  
 921 California air basins. The symbols give the annual ODVs for each air basin, and the solid curves  
 922 indicate the fits of Equation 1 with the parameters from Table 4 to the corresponding ODVs with  
 923 projections to the year 2058. The line segments at right indicate the asymptotes (i.e., the  
 924 parameter  $y_0$ ) toward which the ODVs are converging (six basins to a common value in black,  
 925 and the Salton Sea Air Basin approaching its own limit in its corresponding color). The dashed  
 926 line indicates the NAAQS. The six annotated years in the colors with initials corresponding to  
 927 the respective basins indicate the projected date that the basin ODV will drop to the NAAQS.